Supplementary Information

Mixed ionic-electronic conduction and defect chemistry of $(Na_{0.5}Bi_{0.5}TiO_3)_{1-x}(BiCoO_3)_x$ ($0 \le x \le 0.06$) solid solutions

Fan Yang[1,*], Yunzhu Du[1], Yidong Hu[2], Qiaodan Hu[2], Patrick Wu[3] and Derek C Sinclair[3]

[1] Institute of Fuel Cells, School of Mechanical Engineering, Shanghai Jiao Tong University, 800 Dongchuan Road, Minhang District, Shanghai, 200240, P. R. China.

[2] School of Materials Science & Engineering, Shanghai Jiao Tong University, 800 Dongchuan Road, Minhang District, Shanghai, 200240, P. R. China.

[3] Department of Materials Science and Engineering, University of Sheffield, Sir Robert Hadfield Building, Mappin Street, Sheffield, S1 3JD, UK.

* Corresponding author. fanyang_0123@sjtu.edu.cn

1. XRD patterns of CoO raw material before and after pre-drying

The raw material used for the Co source is CoO. It fully transforms to Co_3O_4 with the spinel structure after heat treatment overnight at 600 °C.

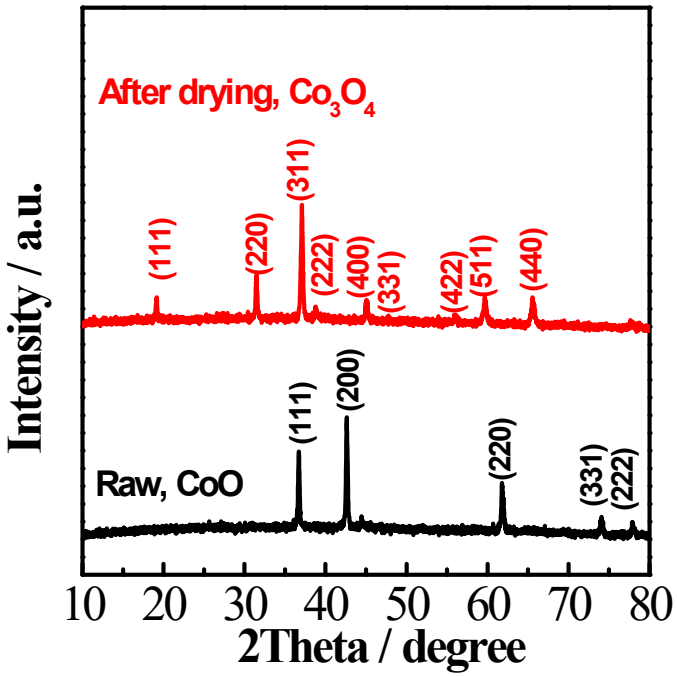

Figure S1. XRD patterns of the raw Co source before and after pre-drying overnight at 600 °C.

2. Impedance spectra for $x = 0.06$

Impedance spectra for $x = 0.06$ show very similar features to those for $x = 0.04$. The major difference identified from the Z^* plot is the absence of an electrode response for this composition (Fig.S2a), which causes noisy C' data in the low-frequency range in the C'-log$f$ plot (Fig.S2c). Combined Z'' and M'' spectroscopic plots (Fig.S2b) show a single M'' peak centered at 79.4 kHz, which is coincident with the Z'' peak, suggesting the single arc on the Z^* plot is the bulk response. Impedance data can be fitted by one R-CPE element, and the σ_b–T^{-1} relationship shows a single $E_a \sim 0.48$ eV (Fig.S2d). Z^* plots for a sample measured in flowing nitrogen, air and oxygen also shows the smallest impedance in nitrogen, and the largest in oxygen, suggesting the presence of n-type electronic conduction (Fig.S2e). An electrode spike can be observed only for samples in nitrogen. Compared with $x = 0.04$, the oxide-ion conduction is suppressed and the electronic contribution is enhanced.

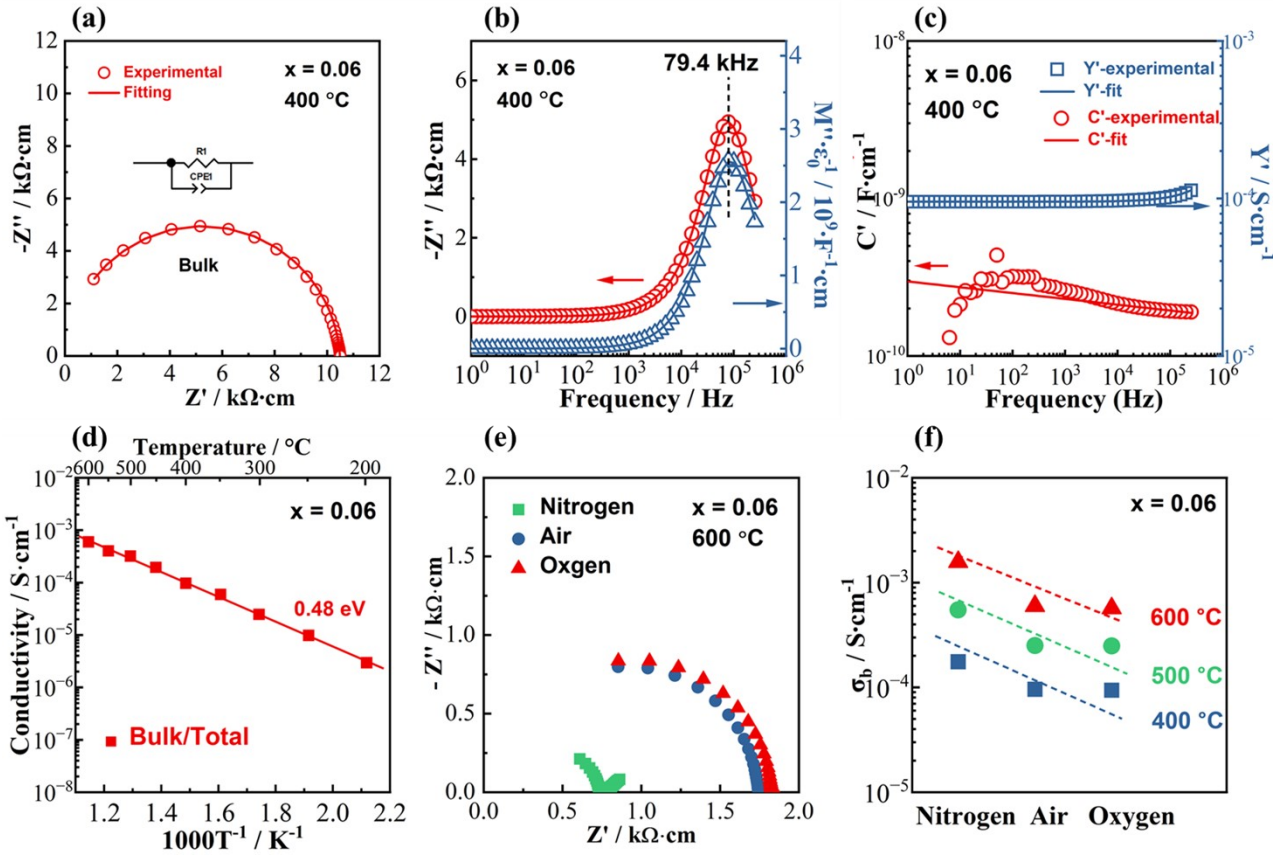

Figure S2. (a) Z^* plot of $(NBT)_{0.94}(BC)_{0.06}$ measured at 400 °C in air. The inset figure is the equivalent circuit for fitting; (b) Combined Z'' and M'' spectroscopic plots; (c) Combined C' and Y' spectroscopic plots; (d) Arrhenius plots of bulk/total conductivity. The number in eV is the activation energy for bulk conduction. (e) Z^* plots for a sample measured in flowing nitrogen, air and oxygen at 600 °C in the frequency range between 1 MHz to 0.01 Hz; (f) Bulk conductivity values under different atmospheres at selected temperatures. The dashed lines serve as guide to the eye.

3. Determination of the upper and lower boundaries for σ_{ion} in Fig.10

Following our "standard" solid-state synthesis and sintering route using rutile as the source of TiO_2, σ_b values of the nominally stoichiometric $NB_{0.50}T$ ceramics vary between ~ 0.5 to 2 $mS \cdot cm^{-1}$ at 600 °C [1-3]. These two values are used as the upper and lower limit for $x = 0$. Our previous experimental studies on NBT-$BiAlO_3$/$BiGaO_3$/$BiScO_3$ solid solutions show that the ability of B-site acceptor dopant to trap oxygen vacancies depends on its ionic size, i.e., smaller ions have stronger ability to trap oxygen vacancies [4, 5]. Therefore, it is assumed that Co^{3+} has similarly strong ability to trap oxygen vacancies as Ga^{3+} due to the similar ionic radius. For the same reason, Co^{2+} has similarly weak ability as Sc^{3+}. Therefore, the slope obtained from linear fitting of the $\sigma_b - x$ relationship of the NBT-BS series represents the weak trapping effect from the large Co^{2+} (Slope 1), and that of the NBT-BG represents the strong trapping effect from the small Co^{3+} (Slope 2). The upper boundary for σ_{ion} is determined by a straight line with Slope 1 passing the highest σ_b for $x = 0$, and the lower boundary is determined by a straight line with Slope 2 passing the lowest σ_b for $x = 0$. Therefore, when the composition factor x varies between 0 and 0.06, the oxide ion conductivity of NBT-BC decreases with increasing x and varies in the pink-shaded region in Fig.10.

4. SEM images for $x = 0.08$ and 0.10

NBT-BC with higher BC contents, $x = 0.08$ and 0.10, were prepared to magnify the effect of Bi-rich grain boundaries and Co-rich particles on the electrical conductivity. SEM images on fracture surfaces and thermally-etched surfaces of the above two compositions are shown in Fig.S3, where Bi segregation on the GBs and Co-rich particles can be clearly observed.

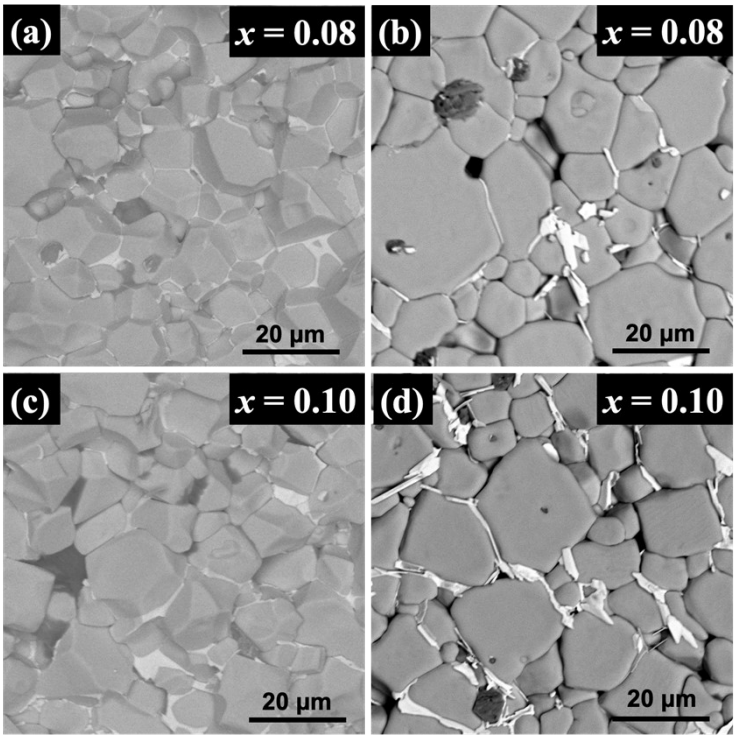

Figure S3. SEM images for x = 0.08 and 0.10. (a) and (c) are on fracture surfaces; (b) and (d) are on polished and thermally-etched surfaces.

5. σ_b-x relationship in the extended Region II

In the extended Region II, where Bi-rich and Co-rich secondary phases can be identified under SEM, σ_b (in log scale) increases almost linearly with increasing x, as shown in Fig.S4.

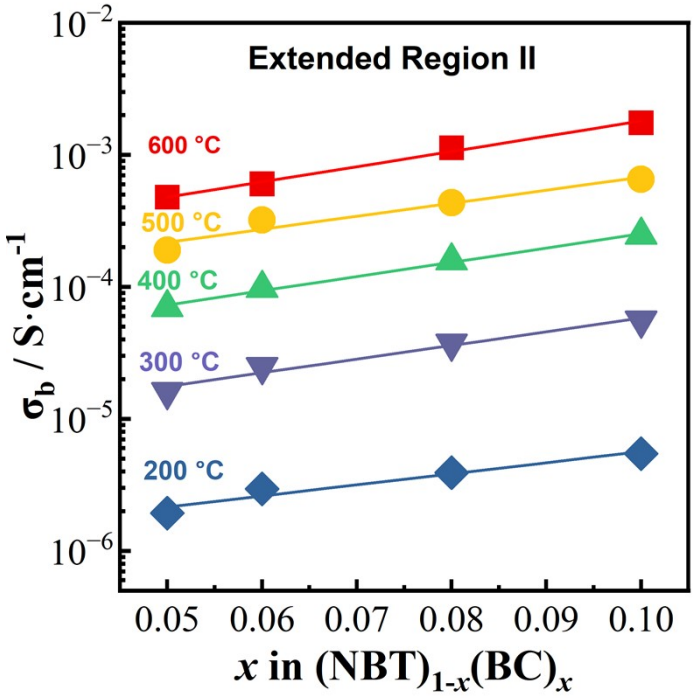

Figure S4. Variation of σ_b as a function of x in the extended Region II (x = 0.05, 0.06, 0.08 and 0.1).

References

[1] F. Yang, Y. Hu, Q. Hu, S. Steiner, T. Frömling, L. Li, P. Wu, E. Pradal-Velázquez, D. C. Sinclair, J. Mater. Chem. A 2022, **10**, 891.

[2] M. Li, M. J. Pietrowski, R. A. De Souza, H. Zhang, I. M. Reaney, S. N. Cook, J. A. Kilner, D. C. Sinclair, Nat. Mater. 2014, **13**, 31.

[3] L. Li, Oxide ion conduction in A-site Bi-containing perovskite-type ceramics, PhD Thesis, The University of Sheffield, 2016.

[4] F. Yang, P. Wu, D. C. Sinclair, J. Mater. Chem. C 2017, **5**, 7243.

[5] F. Yang, P. Wu, D. C. Sinclair, J. Mater. Chem. C 2018, **6**, 11598.